Surface Science of Soft Scorpionates

DOI: 10.1021/ic9014898

Dawn Wallace, Edward J. Quinn, David R. Armstrong, John Reglinski*, Mark D. Spicer, W. Ewen Smith.

WestChem, Department of Pure & Applied Chemistry, University of Strathclyde, 295 Cathedral Street, Glasgow, G1 1XL, U.K.

To whom correspondence should be addressed.

E-mail: j.reglinski@strath.ac.uk/m.d.spicer@strath.ac.uk
Tel 44-141-548-2349/2800
Fax 44-141-548-4822

Abstract

The chemisorption of the soft scorpionate Li[PhTm^{Me}] onto silver and gold surfaces is reported. Surface enhanced Raman spectroscopy in combination with the Raman analysis of suitable structural models; *viz* [Cu(κ^3-S,S,S-PhTm^{Me})(PCy$_3$)], [Ag(κ^3-S,S,S-PhTm^{Me})(PCy$_3$)], [Ag(κ^2-S,S-PhTm^{Me})(PEt$_3$)] and [Au(κ^1-S-PhTm^{Me})(PCy$_3$)] are employed to identify the manner in which this potentially tridentate ligand bind to these surfaces. On colloidal silver SERS spectra are consistent with PhTm^{Me} binding in a didentate fashion to the surface, holding the aryl group in close proximity to the surface. In contrast, on gold colloid, we observe that the species prefers a monodentate coordination in which the aryl group is not in close proximity to the surface.

Introduction

Colloids prepared from silver and gold have become extremely important in analytical biotechnology and trace analysis [1]. Their use in combination with vibrational spectroscopy, particularly surface enhanced resonance Raman spectroscopy (SERRS), allows the detection of analytes such as DNA and explosives present at very low concentrations (~10^{-12} – 10^{-13} M) in complex and heterogeneous samples [2]. However, the detection of these species is highly dependant on the analyte adhering to the roughened metal surface [3]. These interactions are typically sustained by polar forces or the dielectric constant of the surface layer. However, if the analyte does not contain a suitable functional group (e.g. pyridine, benzotriazole) with which it can form a durable interaction with the surface it is common to provide a surface modifier which assists the binding process [1-3]. The nature of the surface modifiers commonly used reflect the nature of the analyte. As such, citrate is widely used for proteins [4], spermine for DNA [5] and thiolates for the fabrication of self assembled monolayers [6]. While citrate and spermine are highly stable species, thiolates can be prone to oxidation and surface migration. Thus, although sulfur donors are acknowledged to be highly compatible with the noble metal surfaces used in many of the current applications of colloid technology, their chemical behaviour can be expected to affect commercial application as the drive for precision, accuracy, reproducibility and longevity increases.

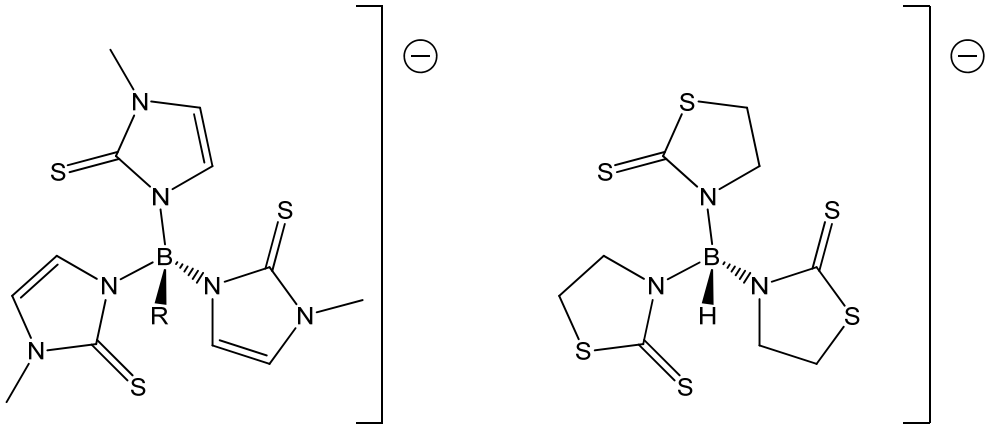

Figure 1. The structure of tris(methimazolyl)borato (R = H, Ph: Tm^{Me}, $PhTm^{Me}$) and tris(thiazolyl)borato anions (Tz) [8].

The unwanted reactivity of the sulfur atom in thiolate based surface modifiers can be reduced by using alternative sulfur based functional groups such as disulfides, thioethers, dithiocarbamates and thiones [7]. The latter attracted our attention some years ago as a result of our interest in the chemistry of sulfur based tripodal thione donors species (Tm^{Me}, Tz; figure 1) [8]. These borate based tripodal species contain a negative charge which is not centred on the sulphur donors. It is thus possible to maintain an interaction between the

thione modifier and the metal surface but to limit the problematic redox properties found in many sulphur donors (e.g. thiolates). Furthermore, these species are polydentate and thus can, potentially, have a larger footprint on the colloid surface than the uni-dentate thiolate species currently used, mitigating problems of modifier migration on the surface.

In our previous study [9] on the use of silver colloid with Tm^{Me} and Tz (Figure 1) we used hemin to show that these species had attached to the surface and that they performed as surface modifiers. Hemin alone is not readily adsorbed onto colloid surfaces and normally does not give surface enhanced Raman spectra. In the presence of our surface modifying ligands, however, surface enhancement was observed suggesting that it interacts with the modifier. It was further inferred that the modifier was bonded to the surface in a didentate mode leaving a thione donor group free to interact with the hemin thus tethering it close enough to the surface for enhancement to occur. Since this preliminary report on the deposition of Tm^{Me} and Tz on silver colloid [9], the chemistry of this ligand system, including their reactions with the coinage metals, has advanced markedly [10, 11]. The coordination chemistry of RTm^{R} with gold, silver and copper indicate that the relationship of the ligand to this group of metals follows the expected trend. It forms monodentate complexes with gold, trigonal and tetradentate complexes with silver and copper. Crucially a small number of novel dimetallic and trimetallic species have now been reported [11]. These complexes are viable models for the manner in which these species might deposit on surfaces whereby the donor thiones distribute themselves amongst adjacent metals. However, this chemistry also suggests that these ligands will interact differently with colloids of different metals.

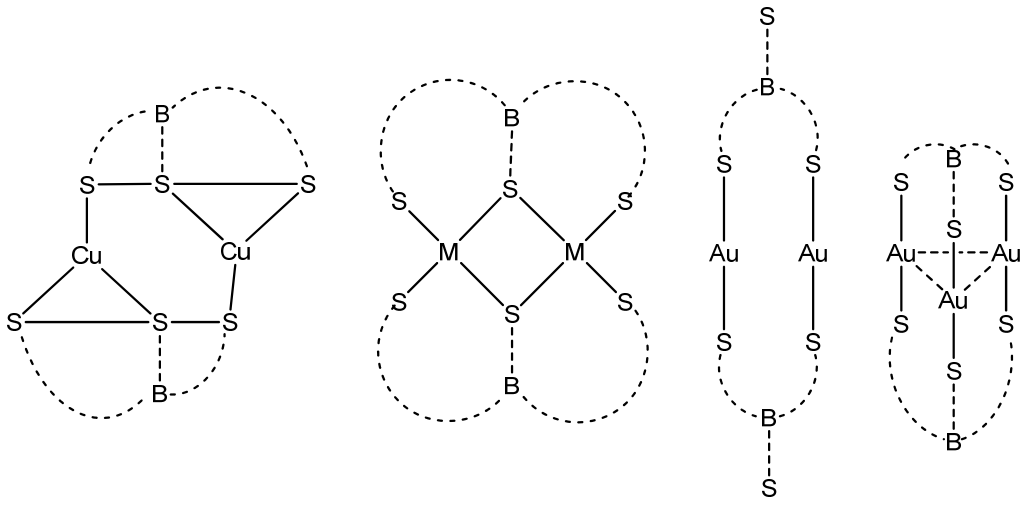

Figure 2. Schematic representations of the di and trimetallic complexes of RTm^{R}. The dotted lines represent the imidazolyl units which connect the boron to the thione donors [11].

Concurrent with our preliminary studies using silver colloid, Santos et al. reported the synthesis of $PhTm^{Me}$ (figure 1) which has an aryl group bonded to the apical boron [12]. This modification introduces a valuable reporting moiety directly onto the boron which should be detected by vibrational analysis. Coupling our increased understanding of the coinage metal coordination chemistry of these species with the availability of a suitable spectral marker, it should now be possible to investigate the deposition of these species on surfaces, assign their complexation modes and probe the differences which occur between gold and silver. The increased footprint of these tripodal species suggested that we should extend this survey to copper in the hope that this material may be stabilised in colloidal form.

Experimental

All experiments were carried out using standard apparatus and commercially available chemicals except for $[Cu(PCy_3)_2Cl]$, $[Ag(PCy_3)_2Cl]$ and $[Au(PCy_3)Cl]$ which were synthesised according to literature methods [13]. Unless otherwise stated reactions and recrystallisations were carried out in air using commercially available solvents and chemicals. ^{1}H and ^{13}C NMR data were acquired at ambient temperature on Bruker DPX or AVANCE NMR spectrometers operating at a proton resonance frequency of 400.13 MHz. Crystals for X-ray analysis were coated in mineral oil and mounted on glass fibres. Data were collected at 120 K on a Nonius Kappa CCD diffractometer using graphite monochromated Mo/Kα radiation. The heavy atom positions were determined by Patterson synthesis (Au) and direct methods (Ag, Cu) and the remaining atoms located in difference electron density maps. Full matrix least-squares refinement was based on F^2, with all non-hydrogen atoms anisotropic. While hydrogen atoms were mostly observed in the difference maps, they were placed in calculated positions riding on the parent atoms. The structure solution and refinement used the programs SHELX-86, SHELX-97 [14] and the graphical interface WinGX [15]. A summary of the crystallographic parameters are shown in Table 1.

Vibrational spectra were collected using either the 514 nm line of a Spectra Physics argon ion laser coupled with a Renishaw inVia Raman microscope or the 632 nm line of a Spectra Physics helium-neon laser coupled with a Renishaw inVia Raman microscope. All spectra were acquired using approximately 20 mW laser power, three 10 second accumulations and a 50× long working distance Olympus microscope objective. Each spectrum was normalised against a silicon reference and baseline corrected using GRAMS software.

Synthesis of [Cu(PhTm^{Me})(PCy$_3$)]: LiPhTm^{Me} (66 mg, 0.15 mmol) was dissolved in MeOH (10 mL) and [Cu(PCy$_3$)$_2$Cl] (100 mg, 0.15 mmol) was added. The reaction was stirred at room temperature for 1 h. The white solid was filtered. Yield: 78 mg, (67%). X-ray quality crystals were grown by slow vapour diffusion of $CHCl_3$/Et_2O. Anal. Calcd. for $C_{36}H_{53}BCuN_6PS_3$: C, 56.05; H, 6.93; N, 10.89. Found: C, 56.01; H, 7.27; N, 10.85. ^{1}H NMR ($CDCl_3$, 400 MHz): δ 7.58 (d, 2H, Ph), 7.25 (m, 3H, Ph), 6.81 (d, 3H, CH), 6.65 (d, 3H, CH), 3.56 (s, 9H, CH_3), 1.78 (br m, 15H, Cy), 1.23 (br m, 15H, Cy). ^{13}C NMR ($CDCl_3$, 100 MHz): δ 162.8 (s, >C=S), 134.9 (s, Ph), 128.2 (s, Ph), 127.1 (s, Ph), 126.7 (s, Ph), 123.4 (s, CH), 117.6 (s, CH), 34.8 (s, CH_3), 32.5 (d, Cy, J(^{31}P, ^{13}C) 44.0 Hz), 30.3 (d, Cy, J(^{31}P, ^{13}C) 16.0 Hz), 27.8 (d, Cy, J(^{31}P, ^{13}C) 44.0 Hz), 26.6 (s, Cy). ^{31}P NMR ($CDCl_3$, 161 MHz): δ -11.3 (br).

Synthesis of [Ag(PhTm^{Me})(PCy$_3$)]: Due to the light sensitive nature of silver compounds the reaction and subsequent crystallisation were carried out in vessels covered with aluminium foil. LiPhTm^{Me} (81 mg, 0.19 mmol) was dissolved in MeOH (10 mL) and [Ag(PCy$_3$)$_2$Cl] (107 mg, 0.15 mmol) was added. The reaction was stirred at room temperature for 12 h. The white solid was filtered. Yield: 101 mg, (65%). X-ray quality crystals were grown by slow vapour diffusion of CH_3CN/Et_2O. Anal. Calcd. for $C_{36}H_{53}AgBPN_6S_3$.½CH_3CN.¼Et_2O: C, 53.55; H, 6.44; N, 10.68; S, 11.29. Found: C, 53.20; H, 7.02; N, 10.77; S, 11.97. ^{1}H NMR (CD_3CN, 400 MHz): δ 7.04 (br m, 2H, Ph), 6.93 (br m, 3H, Ph), 6.62 (br d, 3H, CH), 6.58 (br d, 3H, CH), 3.52 (s, 9H, CH_3), 1.57 (br m, 15H, Cy), 1.22 (br m, 15H, Cy). ^{13}C NMR (CD_3CN, 100 MHz): δ 160.9 (s, C=S), 134.1 (s, Ph), 126.2 (s, Ph), 125.7 (s, Ph), 122.5 (s, CH), 118.8 (s, Ph), 118.2 (s, CH), 34.4 (s, CH_3), 31.2 (d, Cy, J(^{31}P, ^{13}C) = 44.0 Hz), 30.3 (d, Cy, J(^{31}P, ^{13}C) = 19.2 Hz), 26.7 (d, Cy, J(^{31}P, ^{13}C) = 44.8 Hz), 25.7 (s, Cy). ^{31}P NMR (CD_3CN, 161 MHz): δ 34.8 (br d, J(^{31}P, $^{107/109}$Ag) = 1176.1 Hz).

Synthesis of [Au(PhTm^{Me})(PCy$_3$)]: LiPhTm^{Me} (100 mg, 0.23 mmol) was dissolved in MeOH (10 mL) and [Au(PCy$_3$)Cl] (118 mg, 0.23 mmol) was added resulting in a colour change from colourless to orange. The reaction was stirred at room temperature for 1 h. The off white solid was filtered. Yield: 110 mg, (53%). Anal. Calcd. for $C_{36}H_{53}AuBN_6PS_3$: C, 47.79; H, 5.90; N, 9.29; S, 10.63. Found: C, 47.11; H, 6.10; N, 9.19; S, 10.57. ^{1}H NMR ($CDCl_3$, 400 MHz): δ 7.01 (m, 2H, Ph), 6.81 (br m, 3H, Ph), 6.70 (d, 3H, CH), 6.66 (s, 3H, CH), 3.67 (s, 9H, CH_3), 2.07 – 1.75 (br m, 15H, Cy), 1.46 – 1.22 (br m, 15H, Cy). ^{13}C NMR ($CDCl_3$, 100 MHz): δ 134.7 (s, Ph), 126.6 (s, Ph), 126.1 (s, Ph), 124.9 (s Ph), 117.6 (s, CH), 115.6 (s, CH), 35.3 (s, CH_3), 33.6 (d, Cy, J(^{31}P, ^{13}C) = 112.0 Hz), 31.0 (s, Cy), 27.2 (d, Cy,

$J(^{31}P, ^{13}C)$ = 48.0 Hz), 26.0 (s, Cy). The >C=S typically observed at *circa* 160 ppm is too weak to be unequivocally assigned. ^{31}P NMR ($CDCl_3$, 161 MHz): δ 58.2.

Empirical formula	$C_{36}H_{53}BCuPN_6S_3$	$C_{38}H_{54.5}AgBN_{6.5}O_{0.25}PS_3$
Formula weight	771.39	852.19
Temperature	120(2) K	123(2) K
Wavelength	0.71073 Å	0.71073 Å
Crystal system	Triclinic	Triclinic
Space group	P-1	P-1
Unit cell dimensions	a = 9.8533(2) Å α = 90.410(1)° b = 10.0078(2) Å β = 94.723(1)°. c = 19.8773(4) Å γ = 106.028(1)°.	a = 15.0658(2) Å α = 78.009(1)° b = 15.8277(3) Å β = 85.861(1)°. c = 18.2787(4) Å γ = 83.389(1)°.
Volume	1876.59(7) $Å^3$	4230.00(13) $Å^3$
Z	2	4
Absorption coefficient	0.827 mm^{-1}	0.695 mm^{-1}
Reflections collected	37707	37740
Independent reflections	8616 [R(int) = 0.0608]	19400 [R(int) = 0.0367]
Goodness-of-fit on F^2	1.031	0.979
Final R indices [I>2sigma(I)]	R1 = 0.0411, wR2 = 0.0915	R1 = 0.0378, wR2 = 0.0994
No of parameters	436	944

Table 1: Crystallographic data.

Preparation of silver colloid [16]: In a 1000 mL round bottom flask, 500 mL of distilled water was heated to 40°C with a Bunsen burner. A solution of silver nitrate (90 mg in 10 mL distilled water) was added to the water and heated rapidly to 98 °C with constant stirring. Once the solution had reached 98 °C a solution of sodium citrate (110 mg in 10 mL distilled water) was added rapidly, and the solution maintained at 98 °C for 90 minutes with continuous stirring. The nanoparticles produced were consistent with those reported previously (<35 nm diameter) [16]

Preparation of gold colloid [17]: 50 mg of sodium tetrachloroaurate was added to 500 mL of distilled water in a 1000 mL round bottom flask. The solution was heated to boiling point with constant stirring. 7.5 mL of a 1% solution of trisodium citrate was then added. The temperature of the solution was maintained at boiling point for 15 mins and then allowed to

cool to room temperature with continuous stirring. The nanoparticles produced were consistent with those reported previously (15-20 nm diameter) [17]

Surface enhanced resonance Raman spectra. All colloid samples were prepared and analysed in microtitre plates with a sample volume of 250 μL by mixing 30 μL poly-L-lysine (0.01% w/v), 870 μL 50:50 (v/v) colloid: distilled water, and 100 μL 1 x 10^{-2} M ligand solution. Giving a final ligand concentration of 1 x 10^{-3} M.

Density Functional Theory (DFT) molecular orbital calculations: Calculations were performed using the Gaussian 03 program [18]. The molecular species were subjected to geometry optimisation at the DFT [19] level and the 6-311G** basis set [20] for the atoms C, N, O, S, B and H. For Silver, the Stuttgart RSC basis set was used [21]. Preliminary calculations were carried out using the DFT functionals BLYP and B3LYP [22]. The best agreement with respect to the experimental Raman frequencies was obtained using the BLYP functionals and hence these were used for the rest of the molecules.

Results and Discussion

$$Li[PhTm^{Me}] + M(PR_3)_nCl \longrightarrow [M(PhTm^{Me})(PR_3)] + LiCl \qquad -(1)$$

M = Cu, R = cyclohexyl, n = 2: M = Ag, R = cyclohexyl, ethyl, n= 2: M = Au, R = cyclohexyl, n = 1

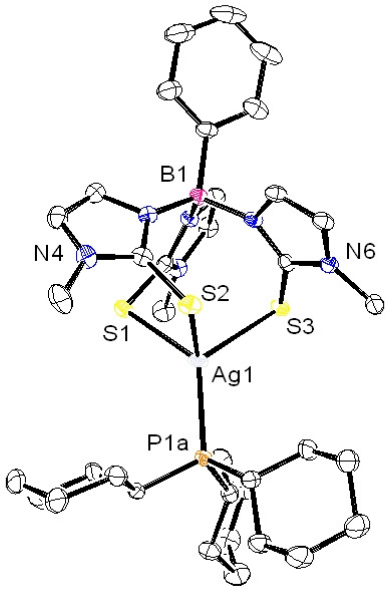

Figure 3. The X-ray crystal structure of [Ag(κ^3-S,S,S-PhTm^{Me})(PCy$_3$)]. The thermal ellipsoids are drawn at 50% probability. The metrical parameters of this complex and its copper analogue can be found in the supplementary material.

A series of model complexes, *viz* [Cu(κ^3-S,S,S-PhTm^{Me})(PCy$_3$)], [Ag(κ^3-S,S,S-PhTm^{Me})(PCy$_3$)], [Au(κ^1-S-PhTm^{Me})(PCy$_3$)] and [Ag(κ^2-S,S-PhTm^{Me})(PEt$_3$)], were initially constructed (eq 1). These complexes were designed to provide representative examples of the manner in which these soft tripodal ligands coordinate with coinage metals. Tricyclohexyl- and triethylphosphine were chosen as supporting ligands in these complexes because the ethyl and cyclohexyl groups are not expected to significantly contribute to the Raman spectra especially in the aromatic region and will not be subject to significant enhancement at the colloid surfaces. Since the chemistry of the coinage metals with these species has previously shown great structural variation [10, 11], it was important to structurally characterise the three new tricyclohexylphosphine (PCy$_3$) adducts prior to their use as surface modifiers.

Both [Cu(PhTm^{Me})(PCy$_3$)] and [Ag(PhTm^{Me})(PCy$_3$)] were readily crystallised allowing for analysis by X-ray methods (figure 3). Both complexes have approximately tetrahedral coordination geometry with the ligand adopting a κ^3-S,S,S coordination mode. The copper complex is iso-structural with its triethylphosphine analogue [10d] whereas the silver complex betrays the ambivalent nature of the heavier element in that the PhTm^{Me} ligand in the triethylphosphine complex is didentate resulting in a trigonal planar geometry at the metal. The relationship between these two silver complexes (PEt$_3$ versus PCy$_3$) is counter-intuitive in that the bulky phosphine displays the higher coordination number. We were unable to obtain suitable crystals of the gold complex, [Au(PhTm^{Me})(PCy$_3$)], for single crystal X-ray diffraction. However, comparisons with the structurally characterised [Au(κ^1-S-Tm^{Me})(PEt$_3$)] using spectroscopic methods clearly supports a linear binding mode for this species.

Solid state Raman spectra of Li[PhTm^{Me}], tricyclohexylphosphine and the four metal complexes [M(PhTm^{Me})(PR$_3$)] (R = Cy, M = Cu, Ag, Au; R = Et, M = Ag) were recorded (figure 4). Using DFT calculations the prominent bands in the Raman spectrum of the [PhTm^{Me}]$^-$ anion were assigned as shown in table 2. Most of the modes are complex in nature, but we have attempted in our assignments to reflect the dominant component. The key vibrational modes are those at 1565 cm^{-1} which is predominantly an aryl C=C stretch [23]; bands a 1371, 1302 and 1283 cm^{-1} which are assigned to C-N stretches in the methimazole rings; a band at 1001 cm^{-1} which is an aryl ring breathing mode; a band at 712 cm^{-1} which arises from N-CH$_3$ stretching and associated methimazole ring breathing; and lastly a band at 535

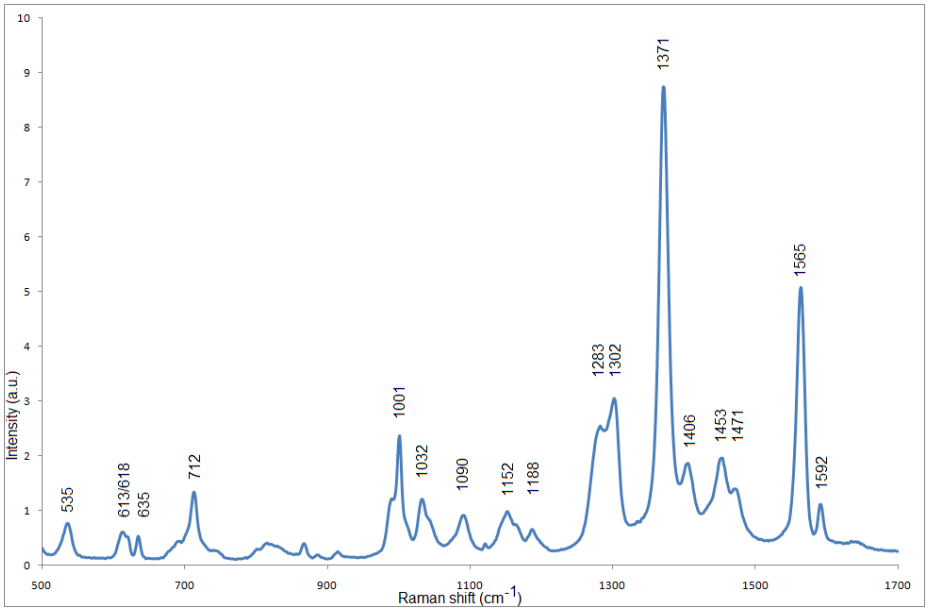
Intensity (a.u.)
Raman shift (cm-1)
535
613/618
635
712
1001
1032
1090
1152
1188
1283
1302
1371
1406
1453
1471
1565
1592

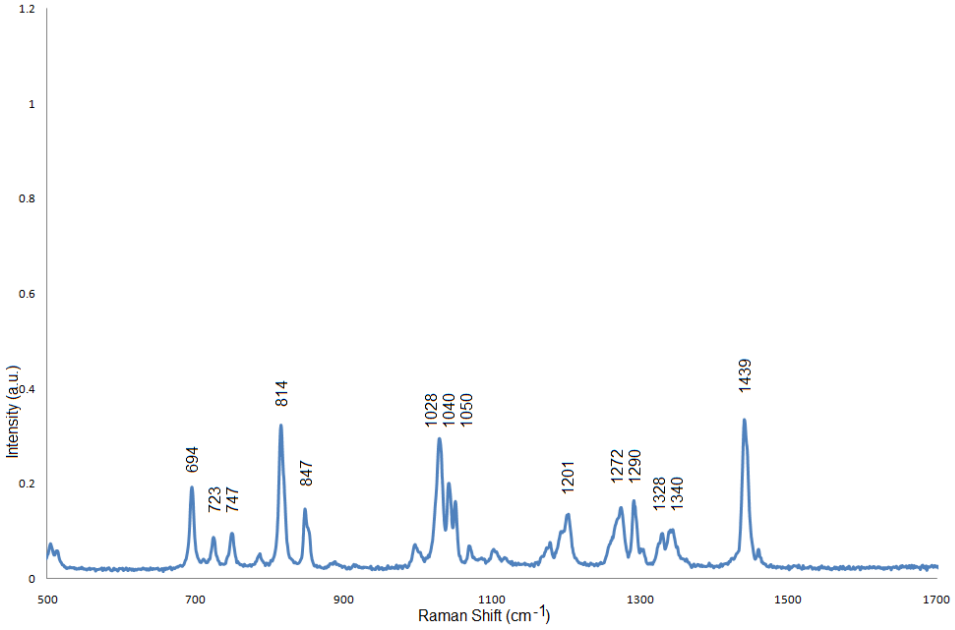
Intensity (a.u.)
Raman Shift (cm-1)
694
723
747
814
847
1028
1040
1050
1201
1272
1290
1328
1340
1439

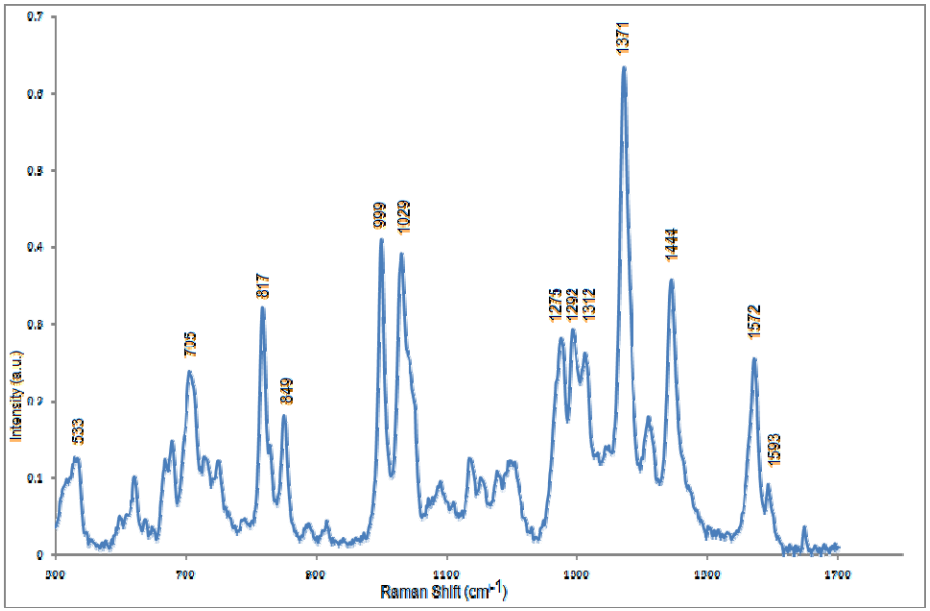
Intensity (a.u.)
Raman Shift (cm-1)
533
705
817
849
999
1029
1275
1292
1312
1371
1444
1572
1593

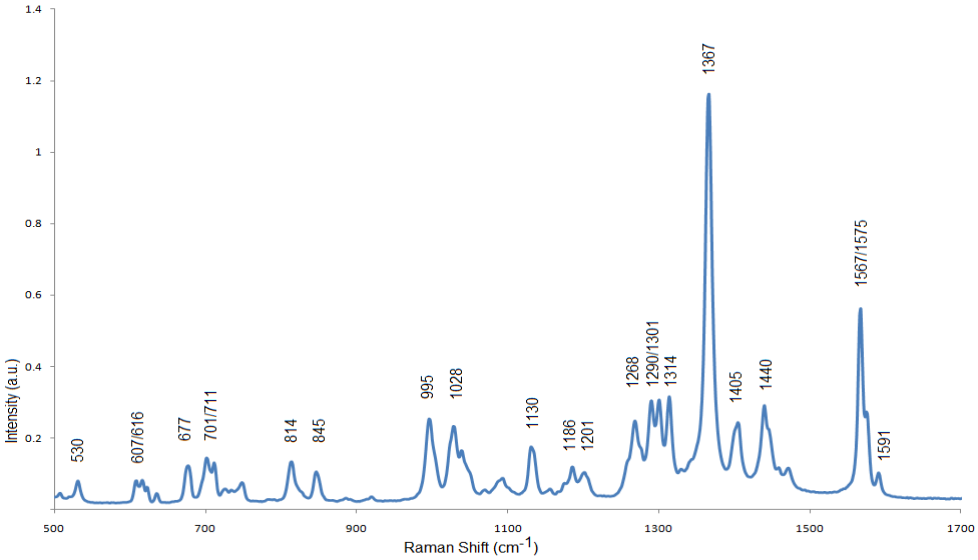
Intensity (a.u.)
Raman Shift (cm-1)
530
607/616
677
701/711
814
845
995
1028
1130
1186
1201
1268
1290/1301
1314
1367
1405
1440
1567/1575
1591

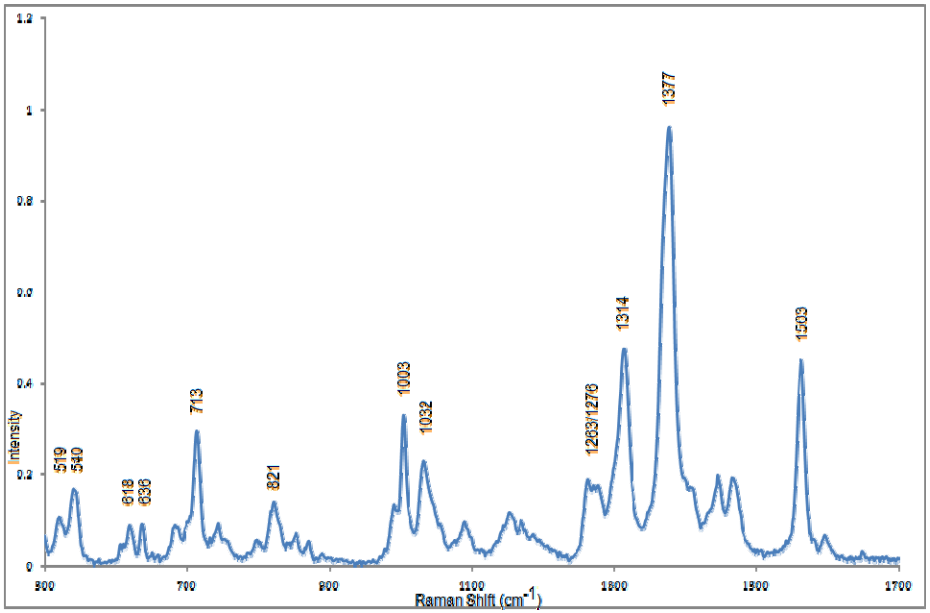

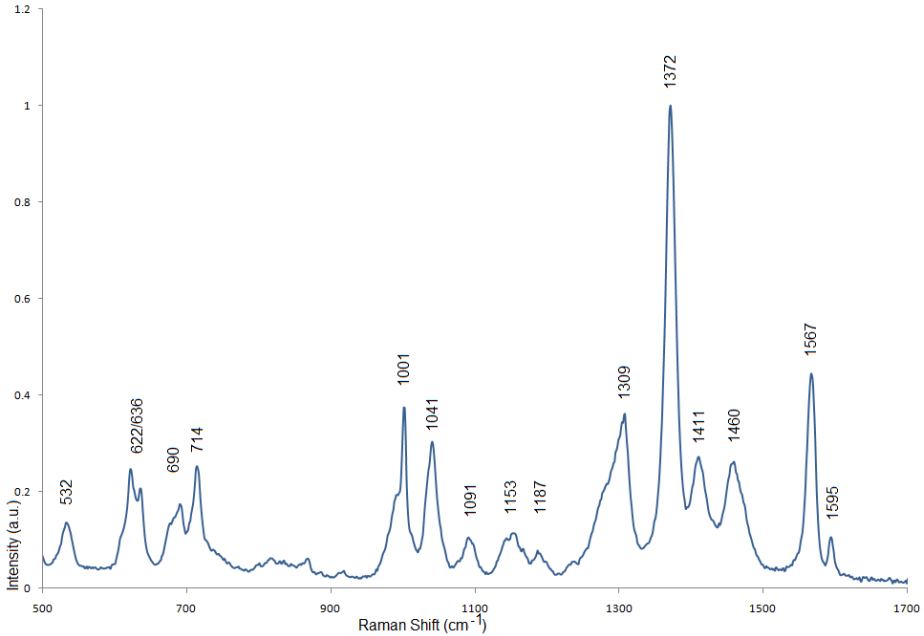

Figure 4 Top left: The Raman spectrum of solid $PhTm^{Me}$, (514 nm, 20 mW). Top right: The Raman spectrum of solid PCy_3, (514 nm, 20 mW). Middle left: The Raman spectrum of solid $[Cu(PhTm^{Me})(PCy_3)]$, (632 nm, 20 mW). Middle right : The Raman spectrum of solid $[Ag(PhTm^{Me})(PCy_3)]$, (514 nm, 20 mW). Bottom left: The Raman spectrum of solid $[Au(PhTm^{Me}(PCy_3)]$, (632 nm, 20 mW). Bottom right; The Raman spectrum of solid $[Ag(PhTm^{Me})(PEt_3)]$, (632 nm, 20 mW).

	ν(C=S) cm^{-1}	ν(N-CH_3)	ν(C=C) (Ph)	ν(C-N) (mt)	Aromatic cm^{-1}
$[PhTm^{Me}]^-$	535	712	1001	1283, 1302, 1371	1565
$Cu(\kappa^3$-S,S,S-$PhTm^{Me})(PCy_3)$	533	705	999	1275,1292,1312,1371	1572
$Ag(\kappa^3$-S,S,S-$PhTm^{Me})(PCy_3)$	530	711	995	1290, 1301, 1314, 1367	1567,1575
$Ag(\kappa^2$-S,S-$PhTm^{Me})(PEt_3)$	532	714	1001	1309 (br) 1372	1567
$Au(\kappa^1$-S-$PhTm^{Me})(PCy_3)$	519,540	713	1000	1263,1276,1314,1377	1563

Table 2. The key vibrational frequencies derived from $PhTm^{Me}$ as the free anion and in its complexes with the coinage metals. The assignments were confirmed using DFT calculations [18-22].

cm^{-1} which is the isolated C=S stretch. The remaining, weaker bands arise from CH_3 deformations (1406, 1453 and 1471 cm^{-1}) and aryl /methimazole C-H bending modes (1032 – 1152 cm^{-1}). It is clear from table 2 that these bands are essentially invariant on complexation, and this has been confirmed by DFT calculations on the silver complexes which show only small shifts in band positions, but do reveal some splitting of bands and changes in intensity. These differences are particularly prominent in the region between 1250 and 1400 cm^{-1} and are also present in the experimental Raman spectra. This is probably due to the changes in symmetry imposed by the different coordination modes of the ligand. In tridentate, κ^3-coordination, these bands are resolved into a group of three/four, whereas for didentate (κ^2) and unidentate (κ^1) forms, which are less geometrically constrained, a broader envelope of bands centred on one dominant frequency is observed.

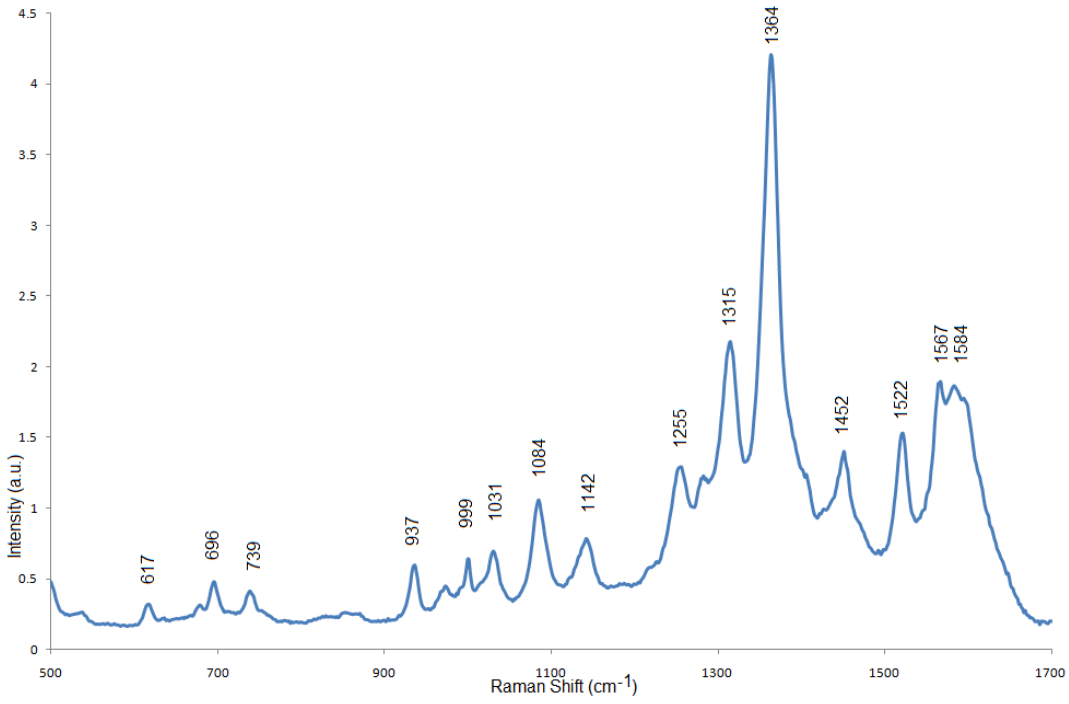

Figure 5 The SERS spectrum of $PhTm^{Me}$ deposited on silver colloid, (514 nm, 20 mW).

Silver colloid was modified by addition of $Li[PhTm^{Me}]$ and the SERS spectrum obtained. The spectrum shows that the thione donor has been chemisorbed on the silver surface (figure 5). The spectrum is again dominated by bands in two frequency ranges namely ca 1300 - 1370 cm^{-1} and ca 1550 - 1650 cm^{-1}. The band due to the >C=S moiety is very weak, possibly occurring at around 500 cm^{-1}, a lower frequency than in the complexes, and on the edge of the observed spectral window. This is in keeping with a significant interaction with the surface. The resonances observed for the methimazole rings appear in the expected

region, however, their number and distribution is reminiscent of the spectrum of [Ag($PhTm^{Me}$)(PEt_3)] thus suggesting a didentate binding mode (figure 4) rather than the tridentate mode observed in the solid PCy_3 complex. Furthermore, comparison of the spectra obtained here for the $PhTm^{Me}$ anion with that reported previously for the Tm^{Me} anion reveals a great deal of similarity between the two species when deposited on the silver surface, again suggesting a didentate binding mode for the Tm^{Me} anion on the silver surface [9]. The relative intensity of the band assigned to the aromatic group is greater on surface deposition and other related vibrations are also enhanced to give a more complex spectrum in this region (figures 4, 5). This implies that the phenyl group is able to approach the surface sufficiently closely for the associated Raman bands to undergo surface enchancement. The additional bands in this region are likely to be other stretching modes of the phenyl ring system which have been selectively enhanced as a consequence of the surface selection rules of SERS. This provides further evidence that this is indeed a SERS rather than a Raman spectrum, a fact already clear from the intensity of what is effectively a monolayer. In the absence of any symmetry considerations, the basic SERS selection rule states that intense scattering arises from vibrations which involve large changes in polarisability perpendicular to the plane of the surface. At about 1600 cm^{-1}, if the plane of the molecule is perpendicular to the surface plane, one mode, a quadrant stretch of the phenyl ring, would be dominant as it is in the Raman spectra of the complexes. The fact that a number of modes are enhanced suggests that the phenyl ring is at an angle to the surface or possibly parallel to it.

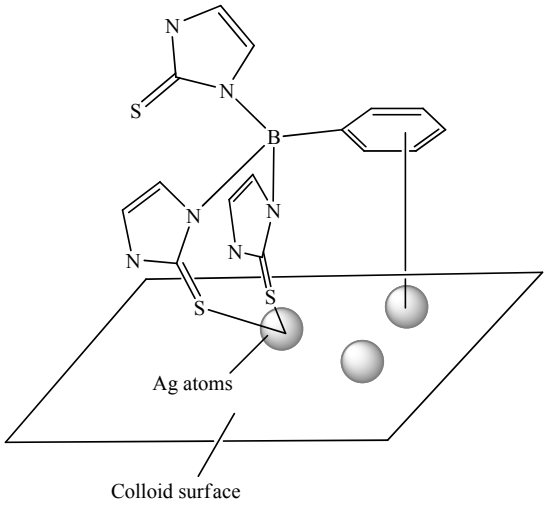

Figure 6. The postulated didentate orientation of $PhTm^{Me}$ on Ag colloid surface which facilitates an interaction of the phenyl moiety with the colloid surface.

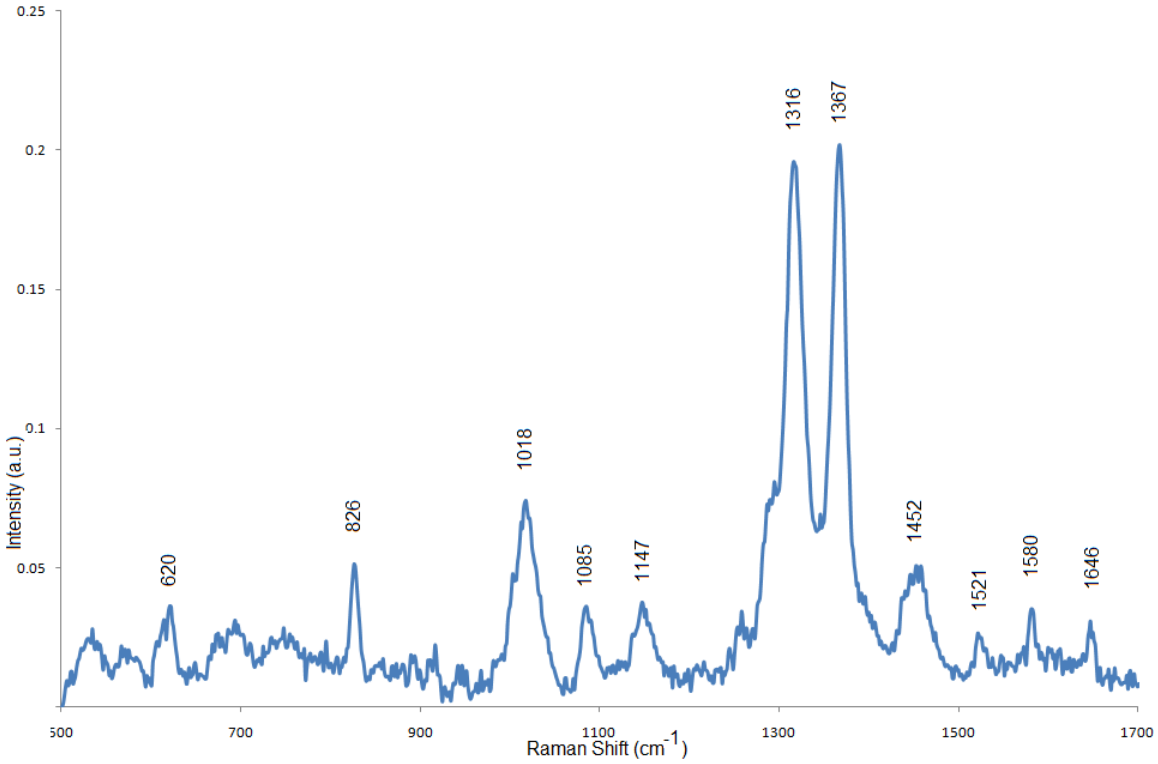

Figure 7 The SERS spectrum of $PhTm^{Me}$ deposited on gold colloid, (632 nm, 20 mW). The lower signal to noise ratio is ascribed to the poorer surface enhancement at gold (c.f. silver)

The SERS spectrum of $PhTm^{Me}$ deposited on gold colloid has only two distinct, high intensity resonances at 1316 cm^{-1} and 1367 cm^{-1}. They are of approximately equal strength, and are assigned to vibrations in the methimazole rings (figure 7). Although the spectrum obtained from $PhTm^{Me}$ deposited on gold colloid and solid $[Au(PhTm^{Me})(PCy_3)]$ have roughly co-incident bands in this region, their absolute and relative intensities have changed, most probably due to the influence of the surface. This would indicate that the structure of the solid gold complex, *i.e.* monodentate and linear, is upheld at the colloidal surface (figure 8). However, this mode of binding potentially allows the phenyl group to come into close proximity with the colloid surface. Thus the absence of a relevant band (~1600 cm^{-1}) suggests that any interaction of this type is very weak due to rapid rotation of $PhTm^{Me}$ on the surface, a process which would be allowed by unidentate coordination. The presence of only one methimazole in close proximity to the surface would also explain the general weakness and breadth of the methimazole bands.

Considering known structures of gold $R'Tm^{R}$ complexes, an alternative model can be envisaged, where each of the three sulfur atoms coordinate to a different gold atom on the colloid surface (figure 8). An overall tridentate coordination mode would be achieved leading

to the phenyl group being remote from the surface, reducing the intensity of the aryl resonance in the SERS spectrum. Coordination of Tm^{R} ligands over three separate gold atoms has been demonstrated by Rabinovich in $[Au_3(Tm^{tBu})_2]^+$ (figure 1) [11c]. However, this mode of binding requires the inversion of the Tm^{Me} ligand at the boron atom forcing the hydridic proton into the core of the metal triangle. This configuration is not possible for $PhTm^{Me}$ (for obvious steric reasons) and the ligand would thus be forced to adopt a configuration with the phenyl group remote from the surface. Such a configuration would be similar to that of the synthetic models, $[Cu(PhTm^{Me})(PCy_3)]$ and $[Ag(PhTm^{Me})(PCy_3)]$ except that three metal centres rather than one would be used to achieve binding. This configuration would have a similar symmetry to the two tridentate complexes and we would thus expect to see a more intense spectrum and bands of disparate intensity between 1300 cm^{-1} and 1380 cm^{-1}. However, this structure would also be highly strained and we consider it unlikely to occur.

In order to probe this further we also obtained the spectrum of the parent Tm^{Me} anion deposited on gold colloid (Figure 9). The spectrum consists of a single intense band at 1372 cm^{-1} accompanied by broad, weak bands at approximately 1327 and 1560 cm^{-1}. This seems more closely allied to the spectrum of the didentate ligand on silver colloid. It is possible that the borohydride can interact with the metal surface [9]. This would be a stronger, more directed interaction than that of the phenyl group in $PhTm^{Me}$ and may result in constraint of the methimazoles close to the surface resulting in a didentate mode.

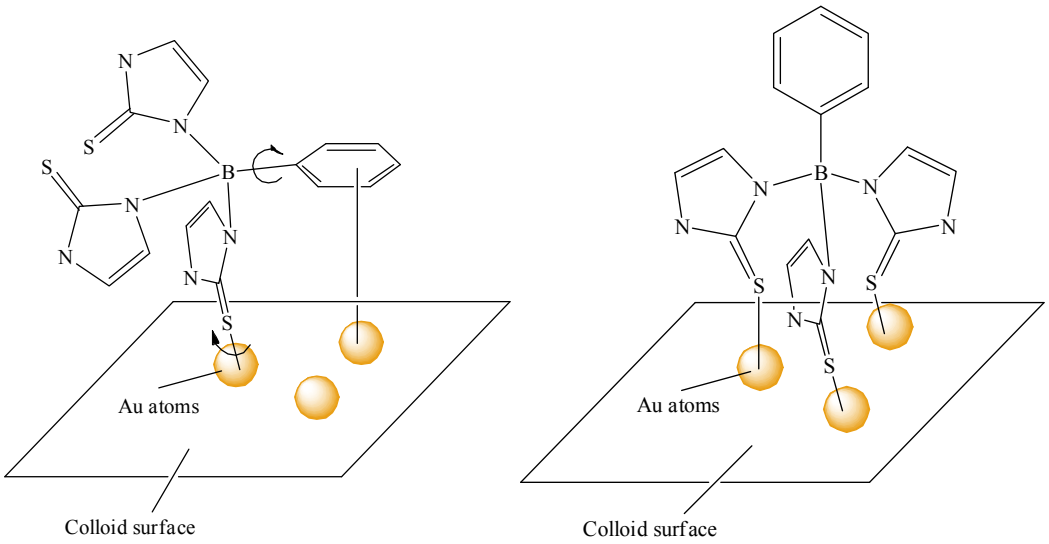

Figure 8. The orientations of $PhTm^{Me}$ on gold colloid surface: (left) monodentate on one individual gold atom, (right) monodentate on three individual gold atoms, with the phenyl moiety remote from the colloid surface.

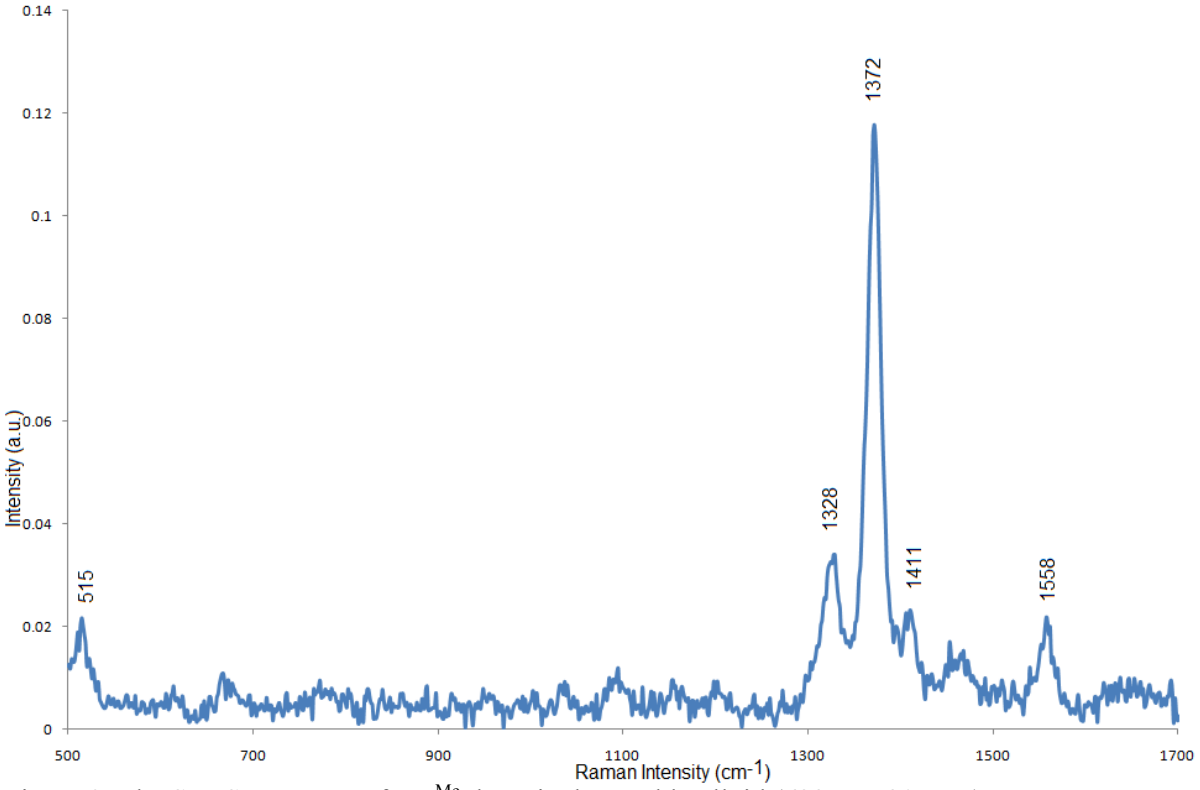

Figure 9. The SERS spectrum of Tm^{Me} deposited on gold colloid (632 nm, 20 mW).

Technologies based on silver and gold colloid are well developed, but copper colloid has not received as much attention due to problems with its stability. We had hoped that the strong affinity of these soft tripodal thione species for copper and their ability to span metal centres (figure 2) would assist the stabilisation of copper colloid. However, despite protracted efforts adding Tm^{Me} and $PhTm^{Me}$ both pre and post colloid formation [24], we were unable to extend the lifetime of this elusive material.

Concluding remarks

The study supports the view that the tripodal thione species $PhTm^{Me}$ and Tm^{Me} are good surface modifiers for silver and gold colloid. However their relationship with the two metal surfaces is different. With gold the surface modifier is unidentate and with silver it is didentate. It is envisaged that eventually the phenyl group will be replaced by a more apposite sensing molecule or a selective coupling agent. Should detection be linked to surface enhancement then the surface of choice would probably be silver as this study predicts that with this material the analyte would be brought into close proximity to the surface.

Acknowledgements

D.W. thanks the EPSRC and University of Strathclyde Doctoral Training Account for financial support.

Supporting Information Available: Crystallographic data for [Cu(κ^3-S,S,S-PhTm^{Me})(P(Cy)$_3$)] and [Ag(κ^3-S,S,S-PhTm^{Me})(P(Cy)$_3$)]. An analysis of the metrical parameters for [Cu(κ^3-S,S,S-PhTm^{Me})(P(Cy)$_3$)], [Ag(κ^3-S,S,S-PhTm^{Me})(P(Cy)$_3$)] and related compounds. Results of DFT studies on PhTm^{Me} and is didentate and tridentate silver complexes leading to an assignment of the vibrational spectrum. This material is available free of charge via the Internet at http://pubs.acs.org.

Footnote

[§]A more complete description of the results of the DFT calculations is given in the supplementary information.

References

1. (a) Ryder, A. G.; O'Connor, G. M.; Glynn, T. J. *J. Raman Spec.* **2000**, *31*, 221-227, (b) Sagmuller, B.; Schwarze, B.; Brehm, G.; Schneider, S. *Analyst* **2001**, *126*, 2066-2071, (c) Faulds, K.; Smith, W. E.; Graham, D.; Lacey, R. J. *Analyst* **2002**, *127*, 282-286.
2. (a) Storhoff, J. J.; Elghanian, R.; Mucic, R. C.; Mirkin, C. A.; Letsinger, R. L. *J. Amer. Chem. Soc.* **1998**, *120*, 1959-1964, (b) Faulds, K.; Smith, W. E.; Graham, D. *Anal. Chem.* **2004**, *76*, 412-417, (c) Faulds, K.; Smith, W. E.; Graham, D. *Analyst* **2005**, *130*, 1125-1131, (d) Faulds, K.; Barbagallo, R. P.; Keer, J. T.; Smith, W. E.; Graham, D. *Analyst* **2004**, *129*, 567-568.
3. (a) Kneipp, K.; Wang, Y.; Dasari, R. R.; Feld, M. S.; Gilbert, B. D.; Janni, J. A.; Steinfeld, J. I. *Spectrochim. Acta A* **1995,** *51*, 2171-2175, (b) Sands, H. S.; Hayward, I. P.; Kirkbride, T. E.; Bennet, R.; Lacey, R. J.; Batchelder, D. N. *J. Forensic Sci*, **1998**, *43*, 509-513, (c) Sylvia, J. M.; Janni, J. A., Klein, J. D.; Spencer, K. M. *Anal. Chem.* **2000**, *72*, 5834-5840, (d) McHugh, C. J.; Keir, R.; Graham, D.; Smith, W. E. *Chem. Commun*. **2002**, 580-581.
4. (a) Rospendowski, B. N.; Kelly, K.; Wolf, C. R.; Smith, W. E. *J. Amer. Chem. Soc*. **1991**, *113*, 1217-1225, (b) Picorel, R.; Chumanov, G.; Cotton, T. M.; Montoya, G.; Toon, S.;

Seibert, M. *J. Phys. Chem.* **1994**, *98*, 6017-6022, (c) Macdonald, I. D. G.; Smith, W. E. *Langmuir* **1996**, *12*, 706-713, (d) Pearman, W. F.; Lawrence-Snyder, M.; Angel, S. M.; Decho, A. W. *Appl. Spec.* **2007,** *61*, 1295-1300.

5. (a) Graham, D.; Faulds, K. *Chem. Soc. Rev.* **2008**, *37*, 1042-1051, (b) Faulds, K.; McKenzie, F.; Smith, W. E.; Graham D. *Angew. Chem. Int. Ed.* **2007**, *46*, 1829-1831, (c) Faulds, K.; Smith, W. E.; Graham, D. *Anal Chem.* **2004**, *76*, 412-417, (d) Graham, D.; Mallinder, B. J.; Smith, W. E. *Biopolymers* **2000**, *57*, 85-91
6. (a) Krolikowska, A.; Bukowska, J. *J. Raman Spec.* **2007**, *38*, 936-942, (b) Srisombat, L. O.; Park, J. S.; Zhang, S.; Lee, T. R. *Langmuir* **2008**, *24*, 7750-7754, (c) Zhang, F.; Skoda, M. W. A.; Jacobs, R. M. J.; Dressen, D. G.; Martin, R. A.; Martin, C. M.; Clark, G. F.; Lamkemeyer, T.; Schreiber, F. *J. Phys. Chem.* **2009**, *113*, 4839-4847.
7. (a) Chung, Y. C.; Chiu, Y. H.; Wu, Y. W.; Tao, Y. T. *Biomaterials* **2005**, *26*, 2313-2324, (b) Mekhalif, Z.; Fonder, G.; Auguste, D.; Laffineur, F.; Delhalle, J. *J. Electroanal. Chem.* **2008**, *618*, 24-32, (c) Ito, E.; Noh, J.; Hara, M. *Surface Sci.* **2008**, *602*, 3291-3296, (d) Long, D. P.; Troisi, A. *J. Amer. Chem. Soc*. **2007**, *129*, 15303-15310, (e) Shervedani, R. K.; Hatefi-Mehrjardi, A.; Babadi, M. K. *Electrochim. Acta* **2007**, *52*, 7051-7060.
8. (a) Reglinski, J.; Garner, M.; Cassidy, I. D.; Slavin, P. A.; Spicer, M. D.; Armstrong, D. R. *J. Chem. Soc. Dalton Trans.* **1999,** 2119-2126, (b) Ojo, J. F.; Slavin, P. A.; Reglinski, J.; Garner, M.; Spicer, M. D.; Kennedy, A. R.; Teat, S. J. *Inorg. Chim. Acta* **2001,** *313,* 15-20, (c) Spicer, M. D.; Reglinski, J. *Eur. J. Inorg. Chem.* **2009**, 1553-1574
9. Reglinski, J.; Spicer, M. D.; Ojo, J. F.; McAnally, G. D.; Skórska, A.; Smith, S. J.; Smith, W. E. *Langmuir* **2003,** ***19,*** 6336-6338.
10. (a) Effendy,; Lobbia, G. G.; Marchetti, F.; Pellei, M.; Pettinari, C.; Pettinari, R.; Santini, C.; Skelton, B. W.; White A. H. *Inorg. Chim. Acta* **2004**, *357,* 4247- 4256, (b) Santini, C.; Pettinari, C.; Lobbia, G. G.; Spagna, R.; Pellei, M.; Vallorani, F. *Inorg. Chim. Acta* **1999**, *285,* 81-88, (c) Bailey, P. J.; Dawson, A.; McCormack, C.; Moggach, S. A.; Oswald, I. D. H.; Parsons, S.; Rankin, D. W. H.; Turner, A. *Inorg. Chem.* **2005**, *44,* 8884-8898, (d) Lobbia, G. G.; Pettinari, C.; Santini, C.; Somers, N.; Skelton, B. W. White, A. H. *Inorg. Chim. Acta* **2001**, *319,* 15-22,
11. (a) Patel, D. V.; Mihalcik, D. J.; Kreisel, K. A.; Yap, G. A. P.; Zakharov, L. N.; Kassel, W. S.; Rheingold, A. L.; Rabinovich, D. *Dalton Trans.* **2005**, 2410-2416, (b) Effendy,; Lobbia, G. G.; Pettinari, C.; Santini, C.; Skelton, B. W.; White, A. H. *Inorg. Chim. Acta* **2000**, *308,* 65-72, (c) Patel, D. V.; Kreisel, K. A.; Yap, G. P. A.; Rabinovich, D. *Inorg. Chem. Commun*. **2006**, *9*, 748-750, (d) Dodds, C. A.; Garner, M.; Reglinski, J.; Spicer,

M. D. *Inorg. Chem.* **2006**, *45,* 2733-2741, (e) Minoura, M.; Landry, V. K.; Melnick, J. G.; Pang, K-L; Marchio, L.; Parkin, G. *Chem. Commun*. **2006**, 3990-3992.

12. Garcia, R; Paulo, A; Domingos, A.; Santols, I. *Dalton Trans.* **2003**, 2757-2760.
13. (a) Bowmaker, G. A.; Boyd, S. E.; Hanna, J. V.; Hart, R. D.; Healy, P. C.; Skelton, B. W.; White, A. H. *Dalton Trans*. **2002**, 2722-2730, (b) Bowmaker, G. A.; Effendy; Harvey, P. J.; Healy, P. C.; Skelton, B. W.; White, A. H. *Dalton Trans*. **1996**, 2449-2457, (c) Jones, P.G.; Sheldrick, G. M.; Muir, J. A.; Muir, M. M.; Pulgar, L. B. *Dalton Trans.* **1982**, 2113-2125.
14. (a) Sheldrick, G.M. SHELXS-86. Program for crystal structure solution, University of Gottingen, Germany **1986**, (b) Sheldrick, G.M. SHELXS-97. Program for crystal structure solution, University of Gottingen, Germany **1997.**
15. Farrugia, L. J. *J. Appl. Cryst* **1999,** *32*, 837-838.
16. (a) Lee, P. C.; Meisel, D. *J. Phys. Chem.* **1982**, *86*, 3391-3395, (b) Munro, C.; Smith, W. E.; Garner, M.; Clarkson, J., White, P.C. *Langmuir* **1995**, *11*, 3712-3720, (c) Rodger, C.; Smith, W. E.; Dent, G.; Edmondson, M. *Dalton Trans.* **1996**, 791.
17. Grabar, K. C.; Freeman, R. G.; Hommer, M. B.; Natan, M. J. *Anal. Chem.* **1995**, *67*, 735-743.
18. Gaussian 03, revision B.05, M.J. Frisch, G.W. Trucks, H.B. Schlegel, G.E. Scuseria, M.A. Robb, J.R. Cheeseman, J.A. Montgomery Jr., T. Vreven, K.N. Kudin, J.C. Burant, J.M. Millam, S.S. Iyengar, J. Tomasi, V. Barone, B. Mennucci, M. Cossi, G. Scalmani, N. Rega, G.A. Petersson, H. Nakatsuji, M. Hada, M. Ehara, K. Toyota, R. Fukuda, J. Hasegawa, M. Ishida, T. Nakajima, Y. Honda, O. Kitao, H. Nakai, M. Klene, X. Li, J.E. Knox,. H.P. Hratchian, J.B. Cross, V. Bakken, C. Adamo, J. Jaramillo, R. Gomberts, R.E. Stratmann, O. Yazyev, A.J. Austin, R. Cammi, C. Pomelli, J.W. Ochterski, P.Y. Ayala, K. Morokuma, G.A. Voth, P. Salvador, J.J. Dannenberg, V.G. Zakrzewski, S. Dapprich, A.D. Daniels, M.C. Strain, O. Farkas, D.K. Malick, A.D. Rabuck, K. Raghavachari, J.B. Foresman, J.V. Ortiz, Q. Cui, A.G. Baboul, S. Clifford, J. Cioslowski, B.B. Stefanov, G. Liu, A. Liashenko, P. Piskorz, I. Komaromi, R.L. Martin, D.J. Fox, T. Keith, M.A. Al-Laham, C.Y. Peng, A. Nanayakkara, M. Challacombe, P.M.W. Gill, B. Johnson, W. Chen, M.W. Wong, C. Gonzalez, J.A. Pople, Gaussian, Inc. Wallingford CT, 2004.
19. Kohn, A. D. Becke. R. G. Parr, *J. Phys. Chem.*, **1996**, *100*, 12974.
20. (a) A. D. McLean. G. S. Chandler, *J. Chem. Phys*. **1980**, *72*, 5639. (b) R. Krishnan, J. S. Binkley, R. Seeger, J. A. Pople, *J. Chem. Phys*. **1980**, *72*, 650.

21. (a) M. Dolg, H. Stoll, H. Preuss, R. M. Pitzer, *J. Phys. Chem.* **1993**, *97*, 5852. (b) Basis sets were obtained from the Extensible Computational Chemistry Environment Basis Set Database, Version 02/25/04, as developed and distributed by the Molecular Science Computing Facility, Environmental and Molecular Sciences Laboratory which is part of the Pacific Northwest Laboratory, P.O. Box 999, Richland, Washington 99352, USA, and funded by the U.S. Department of Energy. The Pacific Northwest Laboratory is a multi-program laboratory operated by Battelle Memorial Institute for the U.S. Department of Energy under contract DE-AC06-76RLO 1830. Contact David Feller or Karen Schuchardt for further information. http://www.emsl.pnl.gov/forms/basisform.html.
22. (a) A. D. Becke, *Phys. Rev. A.* **1988**, *38*, 3098. (b) C. T. Lee, W. T. Yang, R. G. Parr, *Phys. Rev. B.* **1998**, *37*, 785.
23. The calculations show some methimazole C=C stretching character in the band at 1565 cm^{-1}, but in the parent Tm^{Me} spectrum the bands in this region of the spectrum are very weak. We believe that in the present case it is likely that these bands are predominantly phenyl C=C stretching in character.
24. Creighton, J. A.; Alvarez, M. S.; Weltz, D. A.; Garoff, S.; Kim, M. W. *J. Phys. Chem.* **1983**, *87*, 4793-4799

Soft Scorpionates for surface Science: Supplementary material

Dawn Wallace, Edward J. Quinn, John Reglinski*, Mark D. Spicer, W. Ewen Smith
WestChem, Department of Pure & Applied Chemistry, University of Strathclyde, 295 Cathedral Street, Glasgow, G1 1XL, U.K.

Structural Analysis of [Cu(κ^3-S,S,S-PhTm^{Me})(P(Cy)$_3$)], [Ag(κ^3-S,S,S-PhTm^{Me})(P(Cy)$_3$)] and related compounds.

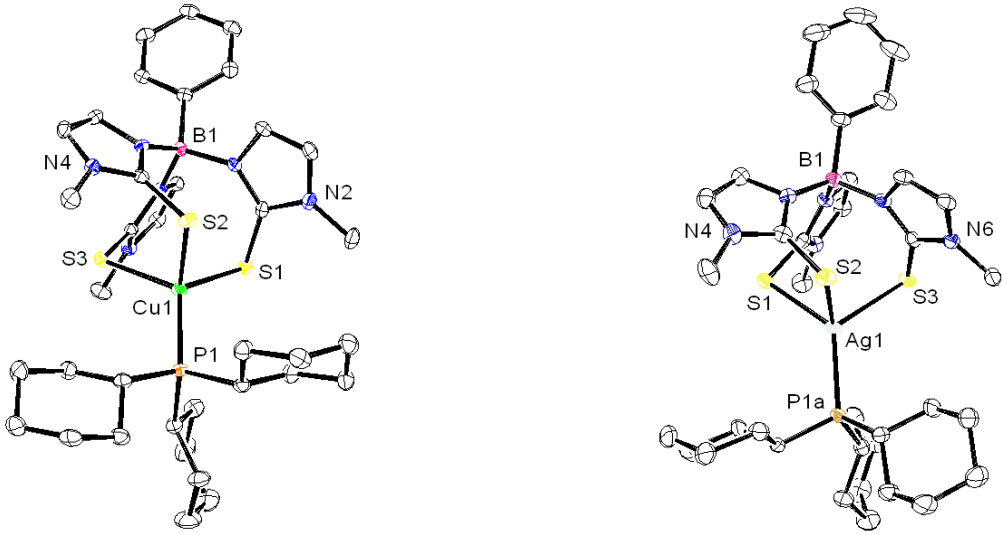

Figure S1. The X-ray crystal structures of [Cu(PhTm^{Me})(PCy$_3$)] (left) and [Ag(PhTm^{Me})(PCy$_3$)] (right, hydrogen atoms omitted for clarity). Selected bond lengths (Å) and angles(º) for these complexes and the related M(Tm)PR$_3$ species can be found in table S1: Additional bond angles for copper: S(1)-Cu-S(2)103.67(2), S(1)-Cu-S(3) 104.13(2), S(2)-Cu-S(3) 98.69(2) and silver; S(1)-Ag-S(2) 96.33(2), S(1)-Ag-S(3) 97.07(2), S(2)-Ag-S(3) 99.13(2).

X-ray crystallography analysis reveals that both Cu(PhTm^{Me})(PCy$_3$) and Ag(PhTm^{Me})(P(Cy)$_3$ (Figure S1) have pseudo-tetrahedral geometry (S$_3$P) with the ligand adopting a κ^3-*S,S,S* conformation. The analogous [Cu(PhTm^{Me})(PPh$_3$)] complex has been previously synthesised and also has pseudo-tetrahedral geometry [11d]. The [Cu(PhTm^{Me})(PPh$_3$)] complex exhibits a high degree of asymmetry which is reflected in the inequivalence of the Cu-S bond lengths (table S1). In comparison, the complex reported here is more symmetrical with all the Cu-S distances being essentially equal, a situation that is also observed in the analogous [Cu(Tm^{Me})(PR$_3$)] complexes (where PR$_3$ = P(*o*/*m*-tolyl)$_3$) [10d] along with Bailey's [Cu(Tm^{Et})(PPh$_3$)] [10c] and Patels's [Cu(Tm^{tBu})(PPh$_3$)] complexes [11a]. In contrast to Cu(PhTm^{Me})(P(Cy)$_3$, the κ^3-*S,S,S* motif is somewhat unusual for silver. Both [Ag(Tm^{Me})(PCy$_3$)] [10b] and [Ag(PhTm^{Me})(PEt$_3$)] [11d] have been previously synthesised

and exhibit the more common didentate coordination (table S1). The [Ag(Tm^{Me})(PCy_3)] complex has an interaction from the hydride moiety which is attributed to the bulky PCy_3 ligand preventing the third sulfur atom from coordinating. Replacement of the BH moiety with a phenyl group in $PhTm^{Me}$ evidently eliminates the possibility for hydride interaction, however, the electronic and steric effect of the ligand alone do not impose κ^3 coordination, as is observed in the [Ag($PhTm^{Me}$)(PEt_3)] complex [11d], where the ligand remains coordinated in κ^2 mode. Peculiarly, the complex reported here incorporates both the $PhTm^{Me}$ ligand and the bulky PCy_3 coligand, producing a complex with tridentate coordination, indicating that there is a subtle relationship between the RTm^{Me} ligand and phosphine auxiliary ligand. The Ag-P bond length in the complex reported here (table S1) is typical of such complexes. As is seen in the analogous complexes there is a degree of asymmetry with the Ag-S distances of 2.5692(8), 2.6337(8) and 2.6381(7) Å being observed. However, these bond lengths are similar to those observed in the analogous [Ag(Tm^{Me})(PCy_3)] and [Ag($PhTm^{Me}$)(PEt_3)] complexes (table S1) [10b, 11d].

	Coord Mode	M-S (Å)	M-P (Å)	<S-M-P (^{o})	ref
Cu(Tm^{Me})P(^{m}Tol)$_3$	κ^3-S,S,S-	2.357	2.217	114.00	10d
Cu(Tm^{Me})P(^{p}Tol)$_3$	κ^3-S,S,S-	2.332	2.226	111.75	10d
Cu(Tm^{Et})PPh_3	κ^3-S,S,S-	2.387	2.229	115.83	10c
Cu(Tm^{tbu})PPh_3	κ^3-S,S,S-	2.353	2.221	114.02	11a
Ag(Tm^{Me})P^{i}Pr$_3$	κ^3-S,S,S-	2.595	2.404	118.19	10a
Ag(Tm^{tbu})PPh_3	κ^3-S,S,S-	2.590	2.424	119.90	11a
Ag(Tm^{Me})PCy_3	κ^2-S,S-	2.603	2.420	126.37	10b
		2.581		119.67	
Au(Tm^{tbu})PPh_3	κ^2-S,S-	2.646	2.247	102.98	11a
		2.349		159.30	
Cu($PhTm^{Me}$)PPh_3	κ^3-S,S,S-	2.352	2.199	109.95	11d
		2.354		111.06	
		2.410		120.31	
Ag($PhTm^{Me}$)PEt_3	κ^2-S,S-	2.463	2.378	124.85	11d
		2.587		135.86	
Au($PhTm^{Me}$)PEt_3	κ^1-S-	2.333	2.268	171.54	11d
Cu($PhTm^{Me}$)PCy_3	κ^3-S,S,S-	2.3842(6)	2.2268(6)	118.98(2)	This
		2.3762(6)		110.28(2)	work
		2.3889(6),		118.34(2)	
Ag($PhTm^{Me}$)PCy_3	κ^3-S,S,S-	2.5692(8)	2.3959(8)	125.89(3)	This
		2.6337(8)		119.39(3)	work
		2.6381(7)		113.77(2)	

Table S1. Tthe metrical parameters around the coinage metal centre for the family of complexes M($RTm^{R'}$)PR_3

Computational Study

In order to make a more definitive assignment of the vibrational spectra of these species, a computational study was undertaken. The the structures of the $PhTm^{Me}$ anion and two fragments, [Ag(κ^2-S,S-$PhTm^{Me}$)] and [Ag(κ^3-S,S-$PhTm^{Me}$)] were optimised and their vibrational spectra calculated. The structures of the optimised fragments are shown below (Figure S2) and the calculated Raman spectra are shown in Figue S3a-c, along with the observed solid state Raman spectra of structurally comparable complexes. The Raman vibrations from the calculated spectra, together with their assignment, are shown in Table S2. The vibrational modes are, on the whole, complex in nature and, although an attempt has been made to describe the major components, they are by no means complete descriptions. The Gaussian 03 output files can be requested from the authors if the reader wishes to inspect these in more detail.

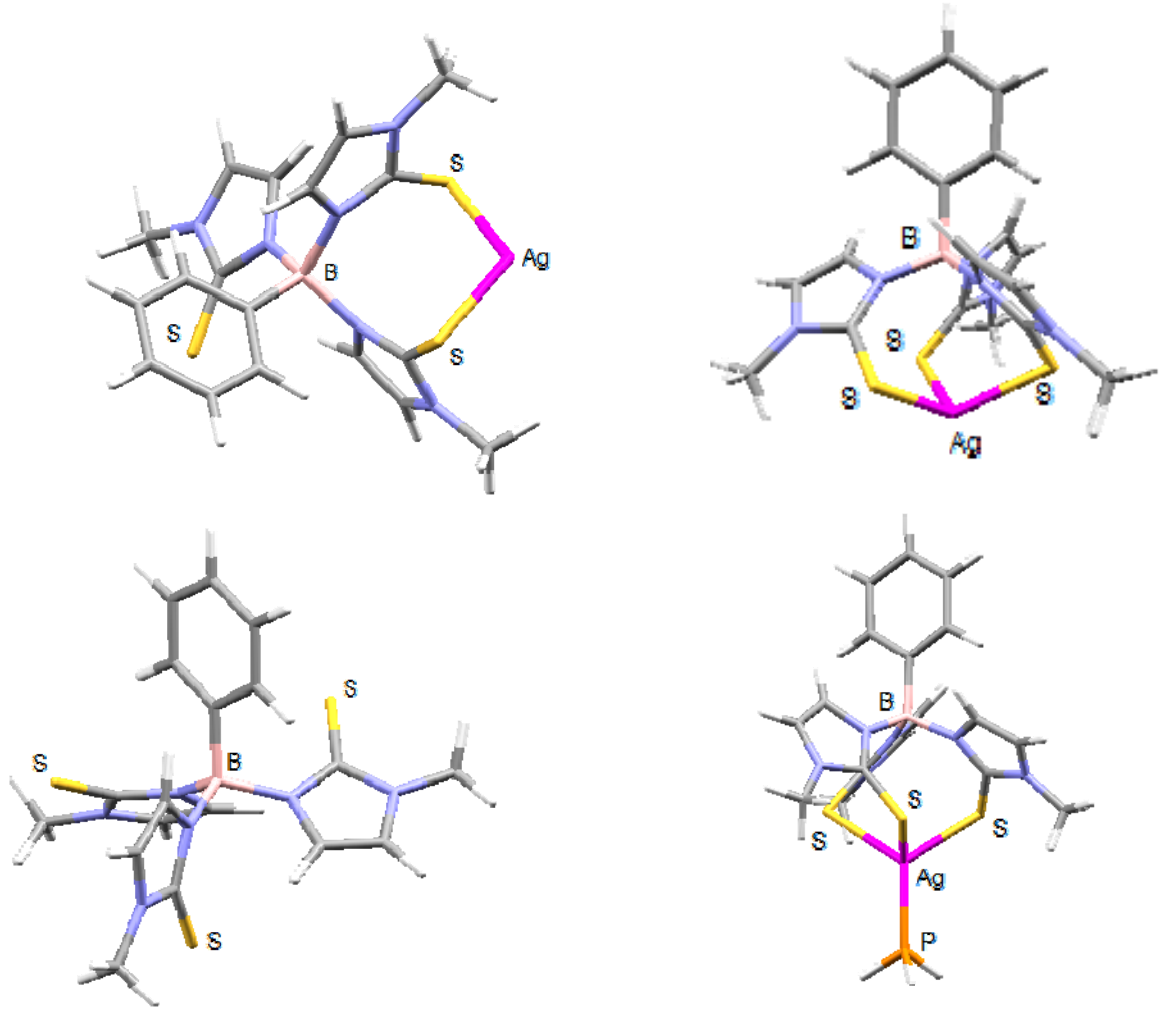

Figure S2: Calculated structures of the $PhTm^{Me}$ anion (below, left), [Ag($PhTm^{Me}$)(PH_3)] (below right) the [Ag(κ^2-S,S-$PhTm^{Me}$)] fragment (above, left) and the [Ag(κ^3-S,S,S-$PhTm^{Me}$)] fragment (above right).

Table S2: Calculated vibrational frequencies (cm^{-1}), correlation with observed bands and assignments.

$PhTm^{Me}$ Calcd	$LiPhTm^{Me}$ Observed	$[Ag(\kappa^2\text{-}PhTm^{Me})]$ Calcd.	$[Ag(PhTm^{Me})(PEt_3)]$ Observed	$[Ag(\kappa^3\text{-}PhTm^{Me})]$ Calcd.	$[Ag(PhTm^{Me})(PCy_3)]$ Observed	$[Ag(PhTm)(PH_3)]$ Calcd	Assignment
523	535	491/495/526	532	509	530	515	ν(C=S)
579	613/618		622/636		607/616		mt out of plane ring deformation
620	635			645		645	mt out of plane ring deformation
699	712	687	690/714	691	677	692	$\nu(N\text{-}CH_3)$/ mt ring breathing
987	1001	988	1001	970/987	995	988	Ph ring breathing
1023	1032		1041	1015/1026	1028	1014/1026	Ph C-H rocking
1068	1090		1091	1070		1071	Ph C-H rocking
						1105	PH_3 P-H bending
1124	1152	1149/1160	1153	1113	1130	1154	mt C-H deformation + ν(C=S)
1202	1188	1192	1187	1201	1186/1201	1208	mt ν(C-N)
				1228	1268	1226	mt ν(C-N)
1265/1272	1283/1301	1261/1273	1309	1267	1290/1301/1314	1268	mt ν(C-N)
1325	1371	1319	1372	1322	1367	1324	mt ν(C-N)
1384	1406	1389	1411	1385	1405	1391	Me H-C-H bending/ mt C-C-H bending
1428	1453	1433/1442	1460	1436	1440	1437	Me H-C-H bending
1480	1471	1475		1477		1477	Me H-C-H bending/ Ph C-C-H bending
1547	1565	1535/1550	1567	1546	1567/1575	1549	Ph ν(C=C) / mt ν(C=C)
1572	1592	1574	1595	1571	1591	1572	Ph ν(C=C)

mtH = methimazole

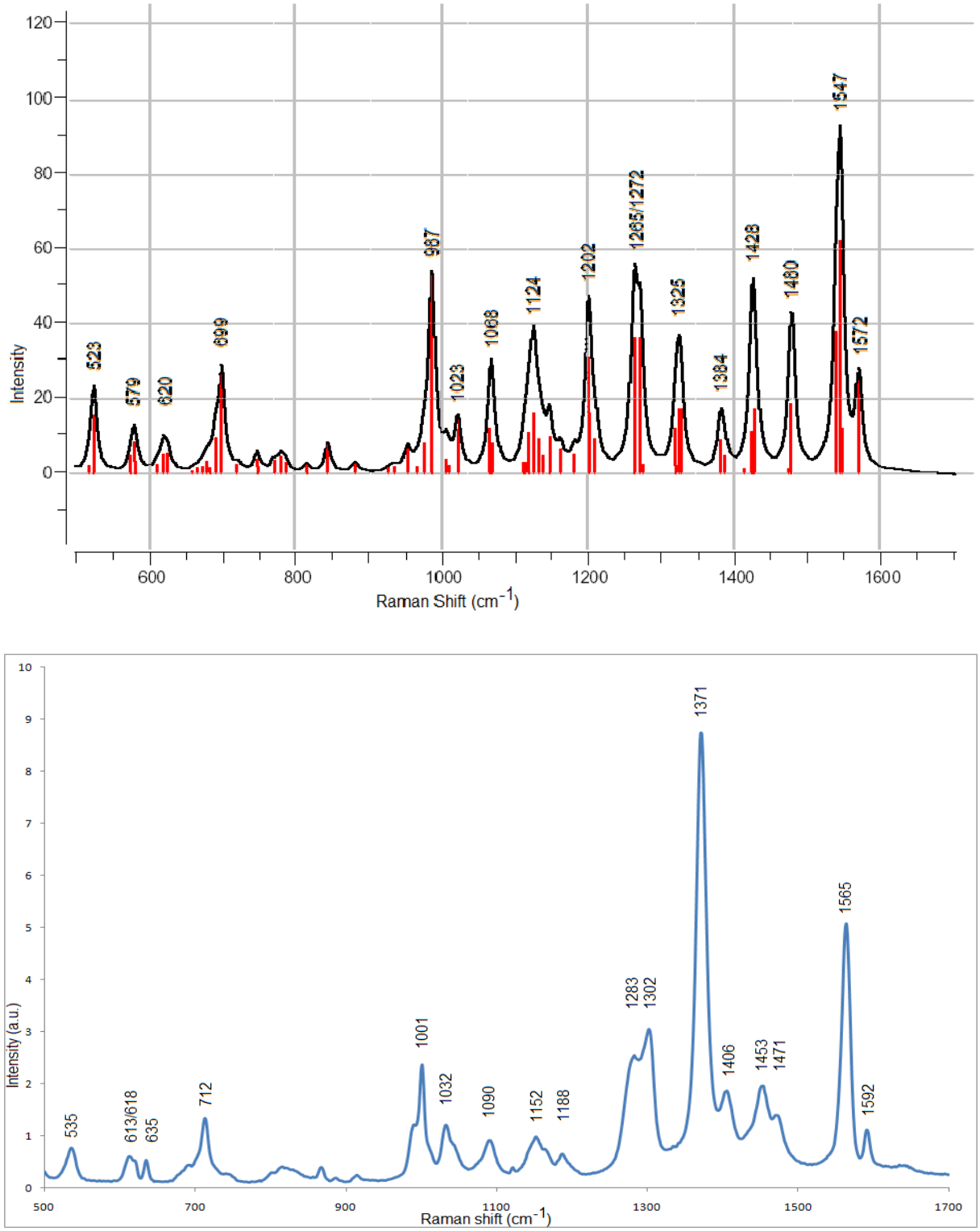

Figure S3a: Calculated (above) and Observed (below) Raman Spectra of $PhTm^{Me}$.

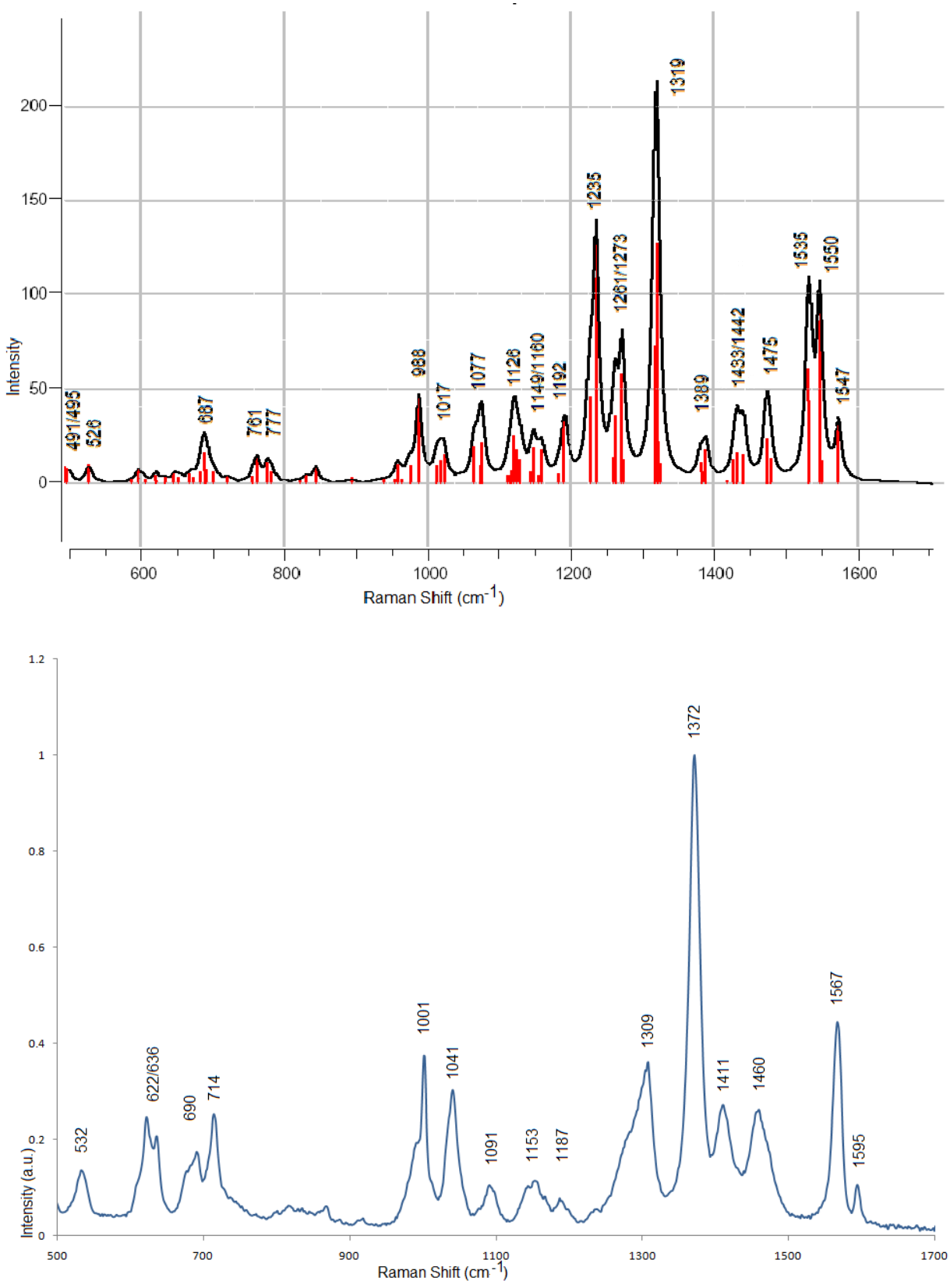

Figure S3b: Calculated Raman Spectrum of [Ag(κ^2-S,S-PhTm^{Me})] (above) and Observed Raman spectrum of [Ag(κ^2-S,S,-PhTm^{Me})(PEt_3)].

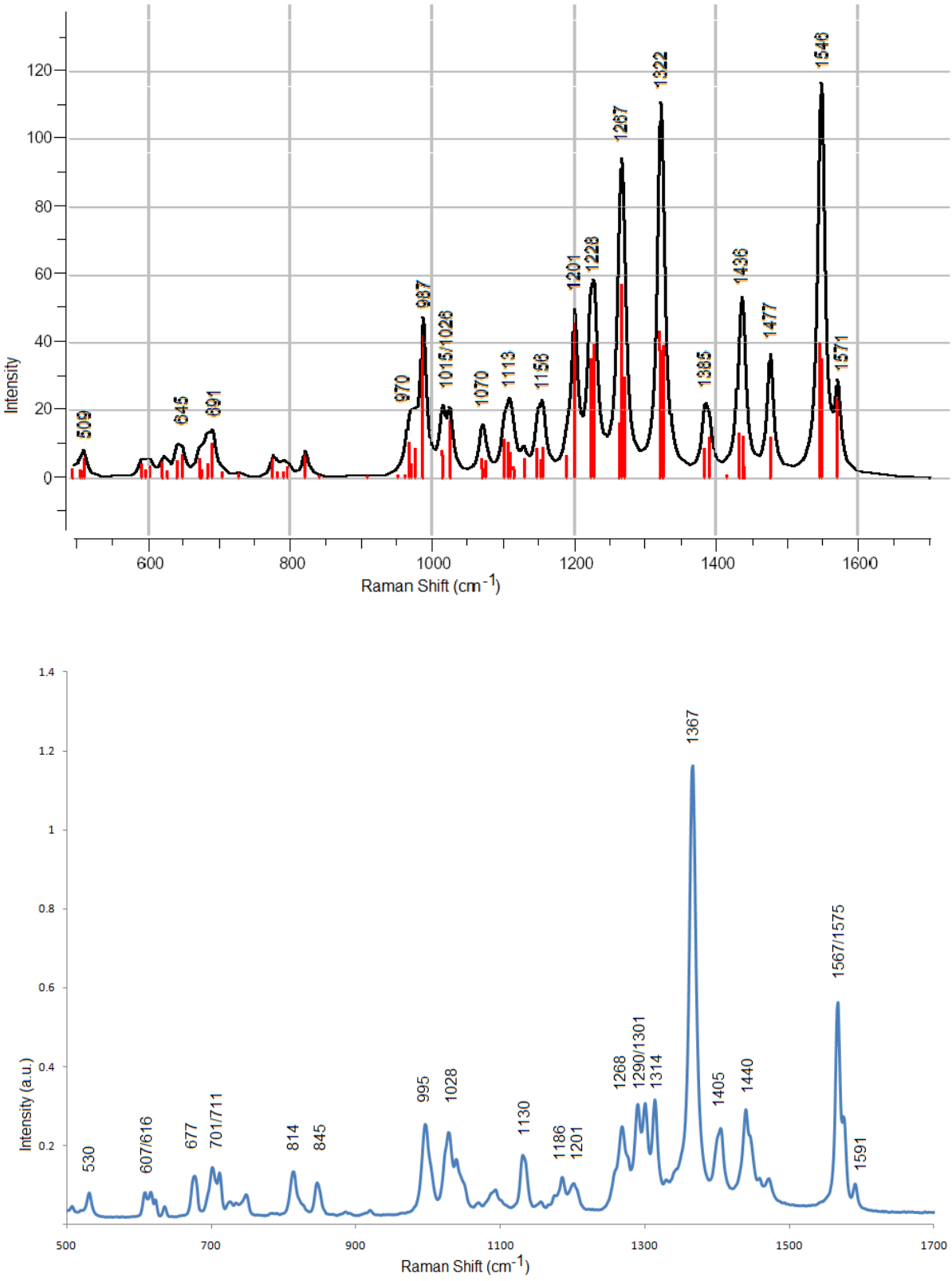

Figure S3c: Calculated Raman Spectrum of [Ag(κ^3-S,S,S-PhTm^{Me})] (above) and the observed Raman spectrum of [Ag(PhTm^{Me})(PCy$_3$)] (below).

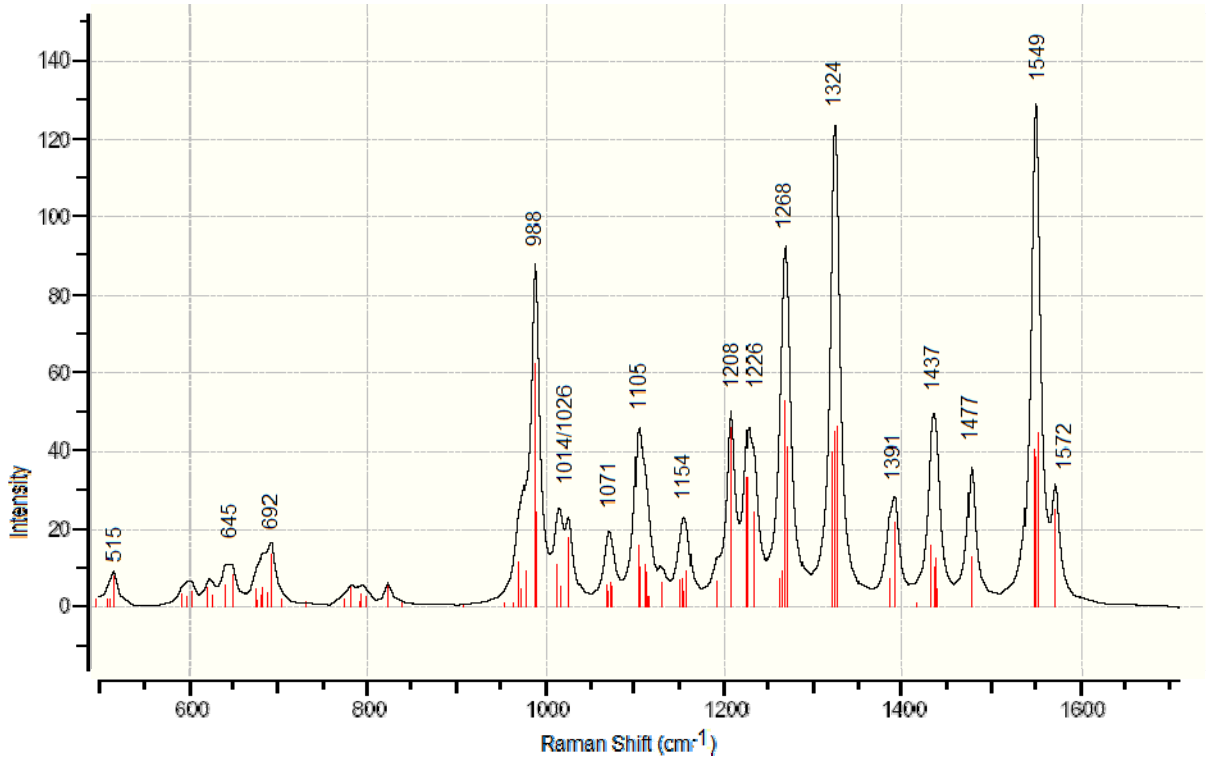

Figure S3d: Calculated Raman spectrum of [Ag(PhTm^{Me})(PH$_3$)].